Progress In Electromagnetics Research, PIER 102, 267–286, 2010

PLANAR TRANSMISSION LINE METHOD FOR CHARACTERIZATION OF PRINTED CIRCUIT BOARD DIELECTRICS

J. Zhang

CISCO Systems, Inc.
CA, USA

M. Y. Koledintseva

Missouri University of Science & Technology
Rolla, MO, USA

G. Antonini

Department of Electrical Engineering
University of L'Aquila
Poggio di Roio, 67040 AQ, Italy

J. L. Drewniak

Missouri University of Science & Technology
Rolla, MO 65401, USA

A. Orlandi

Department of Electrical Engineering
University of L'Aquila
Poggio di Roio, 67040 AQ, Italy

K. N. Rozanov

Institute for Theoretical and Applied Electromagnetics
Russian Academy of Sciences
Moscow 125412, Russia

Corresponding author: M. Y. Koledintseva (marinak@mst.edu).

Abstract—An effective approach to characterize frequency-dispersive sheet materials over a wide RF and microwave frequency range based on planar transmission line geometries and a genetic algorithm is proposed. S-parameters of a planar transmission line structure with a sheet material under test as a substrate of this line are measured using a vector network analyzer (VNA). The measured S-parameters are then converted to ABCD matrix parameters. With the assumption of TEM/quasi-TEM wave propagation on the measured line, as well as reciprocity and symmetry of the network, the complex propagation constant can be found, and the corresponding phase constant and attenuation constant can be retrieved. Attenuation constant includes both dielectric loss and conductor loss terms. At the same time, phase term, dielectric loss and conductor loss can be calculated for a known transmission line geometry using corresponding closed-form analytical or empirical formulas. These formulas are used to construct the objective functions for approximating phase constants, conductor loss and dielectric loss in an optimization procedure based on a genetic algorithm (GA). The frequency-dependent dielectric properties of the substrate material under test are represented as one or a few terms following the Debye dispersion law. The parameters of the Debye dispersion law are extracted using the GA by minimizing the discrepancies between the measured and the corresponding approximated loss and phase terms. The extracted data is verified by substituting these data in full-wave numerical modeling of structures containing these materials and comparing the simulated results with experimental.

1. INTRODUCTION

Development of simple and robust methods for wideband extraction of frequency characteristics of planar sheet materials for various electromagnetic applications is an important present-day problem. In particular, characterization of dielectric substrates for printed circuit boards (PCBs) is vital to achieve the first-pass success in modern high-speed digital system designs. When the on-board data rate is in the Gbps (gigabits per second) range or higher, traces and discontinuities including vias, AC coupling pads, and trace bends on a signal path have to be modeled to catch the channel response accurately [1–3]. A static field solver is not sufficient to model these discontinuities and traces, and full-wave modeling tools have to be used. To build the full-wave model for a given signal path, the detailed structures are known, but the well-represented dielectric material properties of the corresponding substrates are unknown. In general, the dielectric properties (relative

permittivity and loss tangent) used in the full-wave model come from a PCB vendor with only one or two frequency points. However, dielectric representations with either one or two frequency points for a PCB substrate are not sufficient for accurate full-wave simulations, since complex permittivity of a PCB substrate may vary substantially over the wide frequency range. Besides, dielectric representation with only one or two points may result in causality issues in full-wave modeling, which causes the divergence problem in time-domain simulations.

Numerous techniques are known for characterization of dielectric properties over different frequency bands [4–13]. Each technique benefits a different type of materials over a certain frequency range. The resonance techniques widely used in the past several decades to characterize dielectric materials are accurate, but are narrowband [4–6]. Reference [7] extends the resonance techniques to a wideband application by designing a complex structure on a PCB to cover multi-resonant frequency points. The dielectric properties at the corresponding frequency points are tuned by matching the numeric resonant peak to the measurements. The procedure is complicated, and the numerical tuning is cumbersome. In addition, this approach does not measure complex permittivity of a material in the frequency range of interest, since dielectric loss cannot be obtained. As for the coaxial line techniques, they are good for measuring wideband properties of materials homogeneously distributed over the cross-section of the line [8], but they are not suitable for layered materials. Besides, it is difficult to de-embed port effects in this type of techniques. Though it is possible to retrieve dielectric constant and loss tangent of layered materials directly from measurements using an impedance analyzer, this technique is available only at low frequencies with a relatively narrow frequency span [11].

A short-pulse propagation time-domain technique is used to obtain dielectric properties for PCB substrate materials in wide range up to 30 GHz [12]. However, this procedure is complex, while practical manufacturing capabilities and an inherent signal-to-noise ratio of time-domain measurement limit application possibilities as well. A technique for wideband extraction of one-term Debye or Lorentizian behavior of permittivity for PCB substrates directly from frequency-domain S-parameter measurement has been proposed in [13]. It is based on using different planar transmission line structures, and is applied to extraction of dielectric properties up to 5 GHz. Another approach to extract dielectric properties [14] is based on measuring dielectric loss and conductor loss for transmission lines, and it was also tested up to 5 GHz. For an FR-4 material, the approximation of its permittivity by single-term Debye frequency dependence at frequencies

above 10 GHz may be not accurate. It is known that dielectric dispersion of polymer materials can be better approximated by Cole-Cole, Cole-Davidson, or Havriliak-Negami dispersion laws [15, 16]. In addition, it is known that FR-4 type materials can be approximated by so-called "wideband Debye dependence", proposed in [17]. However, this dependence contains logarithms of frequency and is not quite convenient for wideband time-domain numerical modeling, such as FDTD algorithms. Another known way to fit wideband frequency characteristics of such materials is to apply multi-term Debye dependence [17–19],

$$\tilde{\varepsilon}(\omega) = \varepsilon_\infty + \sum_{i=1}^{n} \frac{\chi_i}{1 + \mathrm{j}\omega\tau_\mathrm{i}} - \frac{j\sigma_e}{\omega\varepsilon_0}, \tag{1}$$

where the static susceptibility $\chi_i = \varepsilon_{si} - \varepsilon_\infty$ is the difference between the static relative permittivity and the high-frequency relative permittivity for the ith Debye term, τ_i is the corresponding relaxation constant, ε_0 is the free-space permittivity, and σ_e is the effective conductivity associated with the lowest frequency of interest. This is convenient for representation in numerical codes using time-domain representation.

Even if the dispersion law (e.g., the Debye dependence) for a given dielectric is known, its parameters are typically unknown. Characterization of dielectric materials then can be formulated as an experimental determination of the parameters of the dispersion law without getting the detailed interim information on the values of material parameters over the frequency range of measurements. This allows for simplifying the characterization procedure. In addition, an important requirement for linear passive dielectric materials is compliance with Kramers-Kroenig causality relations [20].

The present paper is aimed at the development of an effective and convenient method to extract parameters of one- and multi-term Debye curves from measurements based on transmission line losses and application of a genetic algorithm (GA). In the past few years, application of GA for solving various electromagnetic problems that require optimization or curve-fitting has gained popularity [21–28], including extraction dielectric properties of materials [13, 14, 29–31]. GA is the most reasonable way of curve-fitting when specifically using rational-fractional functions, such as Debye terms, since it is easily formulated and programmable, robust, efficiently converging to a global minimum. It is important that curve-fitting using rational fractional functions such as the Debye terms provides satisfying Kramers-Kroenig causality relations.

In this paper, the results of extraction are shown for up to two

Debye terms, but an extension for more terms is quite straightforward. The idea of the approach and the GA application are discussed in Section 2. Section 3 contains formulations for different transmission line structures. Three test cases are considered in Section 4. Single-term Debye parameter extraction is demonstrated in a parallel-plate structure and a microstrip structure up to 5 GHz. The parameters of two-term Debye curves are extracted for a stripline structure in the frequency range up to 20 GHz, where one-term Debye curve is insufficient to fit an actual behavior of the dielectric substrates. S-parameters of the structures have been also modeled using full-wave numerical simulations with extracted Debye parameters, and compared with corresponding measurements. Section 5 contains conclusions.

2. PROPOSED APPROACH AND APPLICATION OF A GENETIC ALGORITHM

The approach proposed in the paper to determine parameters of the Debye dispersion law for dielectric substrates includes the following steps: (a) S-parameter measurements, (b) calculation of phase constant β and loss α based on analytical models for the particular transmission lines, (c) comparison between the measured and modeled values of β and α according to some accepted criteria in the frequency range of interest, and (d) correction of the dispersion law parameters until these criteria are satisfied. The correction is fulfilled using a genetic algorithm, which has recently gained popularity for global optimization [21]. This approach is straightforward to extract parameters for a single- or a two-term Debye material. It can also be used for multi-term Debye and more complex dispersion laws [16], including Lorentzian-type characteristics [19, 32], both for permittivity and permeability of magnetic and magneto-dielectric materials. In this method, S-parameters of planar transmission lines (parallel-plate, stripline, and microstrip) with dispersive dielectric substrates are measured using a VNA. The measured S-parameters can be converted into the ABCD matrix parameters, and the complex propagation constant $\gamma = \alpha + j\beta$ in a passive reciprocal network can be calculated as

$$\gamma = \frac{\arccos h\sqrt{A \cdot D}}{l}. \tag{2}$$

if the network is asymmetrical in the general case [33].

The accuracy of the permittivity extraction strongly depends on the accuracy of the measured raw S-parameters, length of the line l, and correct separation of dielectric loss α_d from conductor loss α_c, since total loss is $\alpha = \alpha_c + \alpha_d$. If a zero Through-Reflect-Line (TRL)

calibration is used in the measurement to remove the port effects, the length l is obtained by subtracting the "through" length from the actual length of the test line.

The proposed extraction technique uses a GA optimization. In this technique, the optimization goal is the restoration of the total attenuation α and the propagation constant β, obtained from the measured S-parameters. The evaluated at each frequency point attenuation and propagation constants are related with dielectric properties of substrate through analytical and/or semi-empirical formulas for all the planar transmission lines (parallel-plate, microstrip, and stripline) with a single TEM, or quasi-TEM mode. Interim Debye dielectric parameters are used in each iteration cycle of the GA search. The objective function for optimization is calculated through the root mean square value with respect to all N frequency points

$$\Delta = \frac{1}{N}\sqrt{\sum_{i=1}^{N}\left\{[\Delta_c]^2 + [\Delta_d]^2 + [\Delta_\beta]^2\right\}}, \tag{3}$$

where Δ_c, Δ_d, and Δ_β are the normalized deviations between the measured (with superscript m) and evaluated values (with superscript e)

$$\Delta_c = \frac{|\alpha_c^m - \alpha_c^e|}{\max|\alpha_c^m|}, \quad \Delta_d = \frac{|\alpha_d^m - \alpha_d^e|}{\max|\alpha_d^m|}, \quad \text{and} \quad \Delta_\beta = \frac{|\beta^m - \beta^e|}{\max|\beta^m|}. \tag{4}$$

A fitness index p is assigned to each set of parameters under GA evaluation at that iteration [21]. This index distinguishes how well each individual taken from a solution pool competes with its peers. An individual with a higher p value is much closer to the real solution, and has a higher chance of remaining in the search pool. Based on the fitness index, only "good" individuals are allowed to generate new offspring with higher fitness indices. To maintain diversities in the GA search pool, a small perturbation, or mutation parameter (0.7%) is applied to the new offspring to avoid missing the possible good "genes". As soon as all the chosen criteria are satisfied, the global optimal solutions are reached. Herein, the fitness index is chosen as

$$p = \left(\frac{1}{\Delta}\right)^{1/3}. \tag{5}$$

The power (1/3) in (5) is used to shrink the dynamic range of p, and has been found by extensive numerical experimenting to be a reasonable one for all three geometries — stripline, microstrip, and parallel-plate. We have found that reasonable population size is in the

range of 240–400, and the median value of 320 has been chosen as the optimal population size. The cross-over parameter is chozen as 75%.

Another way to simulate dielectric loss and conductor loss is to assume that the dielectric part is proportional to frequency ($\alpha_d \propto \omega$), while skin-effect part behaves as $\alpha_c \propto \sqrt{\omega}$. This is valid only for perfectly smooth surfaces, while taking into account rough surfaces requires some frequency correction [33, 34]. However, assuming that metal surfaces are basically smooth, the total loss can be approximated as

$$\alpha = a\omega + b\sqrt{\omega}. \tag{6}$$

The coefficients a and b can be retrieved using another genetic algorithm to approximate the dependence $\alpha(\omega)$ retrieved from S-parameter measurements. If surface roughness is included in conductor loss, the frequency dependence of total loss α is more complex than (6), and roughness may contribute to "dielectric" ω-term as well as "smooth conductor" $\sqrt{\omega}$-term, and higher powers of frequency [35]. How to correctly split conductor loss contributions from dielectric loss in a rough conductor is a serious separate problem, and it is beyond the scope of the present paper.

3. FORMULATION FOR PLANAR TRANSMISSION LINES

Analytical or semi-empirical formulas known from literature are used for conversion of complex propagation constant to dielectric parameters of parallel-plate, stripline, and microstrip structures. Though these models are generally approximate, they are accurate enough for dielectric parameter extraction in the frequency range of interest, where TEM (or quasi-TEM) propagation takes place. Limitations of parameter extraction for the transmission line structures under consideration are discussed.

It should be mentioned that though the types of lines, other than those with TEM (quasi-TEM) modes, have not been considered in this particular paper, the presented methodology can be extended to the other regular waveguide structures. It is important that α and β are extracted through measurements, and an adequate model correlating these propagation parameters with dielectric properties of the media under study should be available [36, 37].

3.1. Parallel-plate Structure

A parallel-plate structure shown in Fig. 1 is the simplest transmission line. For the TM_0 mode in the parallel-plate waveguide, $E_z = 0$,

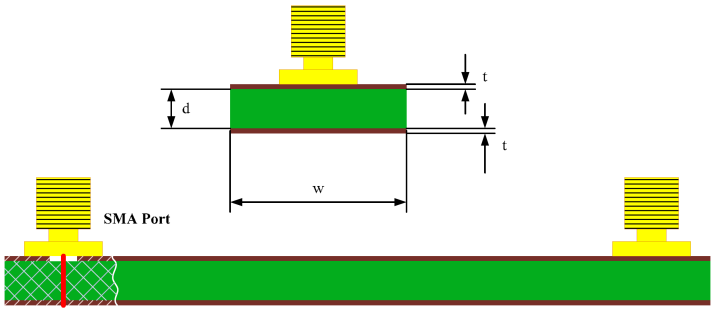

Figure 1. Cross-section of the parallel-plate structure.

and both electric and magnetic fields are transverse to the guidance direction. Therefore, TM_0 mode is also the TEM mode. Since the cut-off frequency of TEM mode is zero, it is often referred to as the lowest (dominant, or fundamental) mode [38].

Formulas for α and β are based on the assumption that the higher order modes and fringing fields are ignored. This is true for a parallel-plate structure only over a limited frequency range, depending on its dimensions and the substrate dielectric. Hence, a set of parallel-plate structures for studying dielectrics in each specific frequency range may be needed. The assumptions given herein imply two rules: (1) the ratio w/d must be large enough, so that the perfect magnetic boundary condition is applicable for neglecting the fringing fields; (2) the cut-off frequency of the first higher-order mode associated with perfect electrical conductor boundary condition limits the thickness d of the dielectric medium between two plates. Thus, the first higher-order modes TE_1 and TM_1 have the cut-off frequency $f_{cut-off} = c_\varepsilon/(2d)$, where c_ε is the wave velocity in the dielectric.

The phase constant for the TEM wave in a parallel-plate transmission line is

$$\beta = \omega\sqrt{\mu_0\varepsilon_0} \cdot \sqrt{\mu_r\varepsilon_r'} \tag{7}$$

where $\mu_r = 1$ is the relative permeability of the non-magnetic substrate material, and ε_r' is the real part of ε_r in (1), which is an interim value during the GA extraction. If conductors of the parallel-plate line are smooth, and if there is the only TEM mode propagating, then the conductor loss is [39]

$$\alpha_c = \frac{R_s}{\eta d}, \tag{8}$$

where $\eta = 120\pi\sqrt{\frac{\mu_r}{\varepsilon_r'}}$ is the TEM wave impedance, $R_s = \sqrt{\omega\mu_0/(2\sigma_c)}$ is the surface resistance of conductors, and d is the thickness of dielectric

substrate. Assuming that the substrate dielectric is low-dispersive and low-loss, the dielectric loss is [39]

$$\alpha_d = \frac{\beta \tan\delta}{2}, \text{ where } \tan\delta = \frac{\varepsilon_r''}{\varepsilon_r'}. \tag{9}$$

If loss and dispersion in a dielectric substrate is considerable loss, then the attenuation constant can be calculated as

$$\alpha_d = \omega\sqrt{\mu_0\varepsilon_0}\sqrt{\varepsilon_r'} \cdot \sqrt[4]{1+(\tan\delta)^2} \cdot \sin(\delta/2). \tag{10}$$

At the same time, the propagation constant will be calculated as

$$\beta = \omega\sqrt{\mu_0\varepsilon_0}\sqrt{\varepsilon_r'} \cdot \sqrt[4]{1+(\tan\delta)^2} \cdot \cos(\delta/2). \tag{11}$$

These formulas are derived from the rigorous expressions for complex propagation constant for TEM wave propagating in a dielectric medium.

3.2. Microstrip Transmission Line

The calculation of α and β for a microstrip line (Fig. 2), is analogous to that for the parallel-plate geometry. Strictly speaking, the electromagnetic field in a microstrip is a hybrid TE-TM mode, and wave propagation is not completely contained within a substrate. However, it can be considered as a quasi-TEM mode for the structures with electrically thin dielectric substrates ($h/\lambda_{diel} \ll 1$). The phase term for the microstrip line filled with a comparatively low-loss dielectric is

$$\beta = \omega\sqrt{\mu_0\varepsilon_0\varepsilon_e'}, \tag{12}$$

where the effective permittivity ε_e' is used instead of real part of permittivity ε_r' for the substrate dielectric. The expression for effective

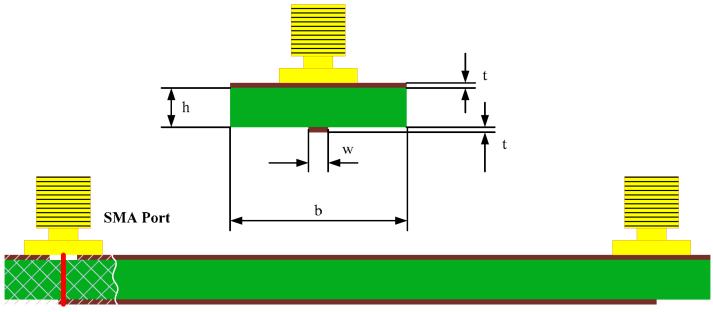

Figure 2. Cross-section of the microstrip structure.

permittivity in a microstrip line can be found in textbooks, for example, [39, P. 162], or [40].

$$\varepsilon'_e = \frac{\varepsilon'_r + 1}{2} + \frac{\varepsilon'_r - 1}{2\sqrt{1 + \frac{12h}{w}}}. \tag{13}$$

The attenuation of the microstrip line due to the finite conductivity in the smooth conductor is

$$\alpha_c = \frac{R_s}{wZ_w}, \tag{14}$$

where $R_s = \sqrt{\omega\mu_0/(2\sigma_c)}$ is the surface resistance of the conductor, and Z_w is the wave impedance of the line [39]. The dielectric attenuation is calculated for the structure as [39]

$$\alpha_d = \frac{\omega\sqrt{\mu_0\varepsilon_0}}{2} \cdot \frac{\varepsilon'_e - 1}{\sqrt{\varepsilon'_e}} \cdot \frac{\varepsilon'_r}{\varepsilon'_r - 1} \cdot \tan\delta, \tag{15}$$

where $\tan\delta = \frac{\varepsilon''_r}{\varepsilon'_r}$ is the loss tangent of the dielectric material. If the dimensions of the structure are known, the total loss $\alpha = \alpha_c + \alpha_d$ and β can be calculated using the above formulas, or through (6). If the material under study is substantially lossy and dispersive, then formulas (10) and (11) should be applied for calculating α and β, but substituting ε'_r with ε'_e in $\tan\delta$. Higher-order modes, surface waves in the metal-dielectric-air structure, and radiation effects in the open dielectric structure are not taken into account, and these factors limit frequency range for permittivity extraction [41].

3.3. Stripline Structure

Equations (7)–(11) can also be used to calculate α and β for a stripline (Fig. 3). If dimensions of a stripline are given, the conductor loss in a

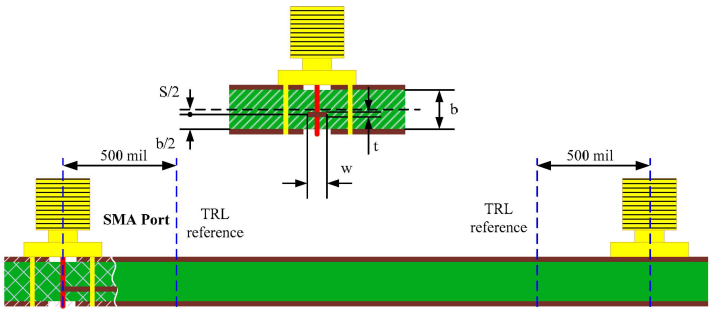

Figure 3. Cross-section of the stripline structure.

smooth conductor can be estimated, for example, using the incremental inductance rule proposed by Wheeler [42, 43]. Wheeler's formulas are valid only for a single TEM mode in a stripline with the assumption of fringing fields and edge coupling negligible. In reality, the higher-order modes can be suppressed by limiting the spacing between the reference plates of the strip to the quarter wavelength ($\lambda/4$). These assumptions are often true in multilayer PCBs, where $t \ll b$ and $b \ll \lambda/4$ (see Fig. 3).

4. MEASUREMENTS AND CASE STUDIES

Three structures have been built and tested. Two structures, parallel-plate and microstrip, made of the same double-sided copper-clad FR-4 sheet have been tested in the frequency range of 100 MHz–5 GHz. This is needed for verifying the consistency while the proposed approach is under validation. Another study is a stripline embedded in an 8-layer PCB. It is shown that an appropriate TRL calibration allows for accurate extracting of two-term Debye curves up to 20 GHz.

4.1. Parallel-plate and Microstrip Transmission Lines

The microstrip and the parallel-plate were made of the copper-clad FR-4 and cut from the same sheet sample. The parallel-plate structure had the dimensions of 71.36 mm (length) × 19.80 mm (width) × 1.25 mm (height). The dielectric spacing (FR-4) was 1.05 mm, and the thickness of the copper was 0.1 mm. Two SMA connectors were symmetrically mounted at the both ends of the structure in the long direction, and the distance between the centre conductors of the SMA was 63.4 mm. The dimensions of the microstrip line with the identical FR-4 material were 69.00 mm × 19.80 mm × 1.25 mm, and the distance between the centre conductors of the two SMA connectors was 61 mm.

S-parameters were measured using an *HP 8753D* VNA in the frequency range of 100 MHz–5 GHz with 1601 sampling frequency points. Prior to the measurements, SOLT ("Short-Open-Load-Through") calibration was implemented. The impact of the electrical length of the SMA connectors upon the measured *S*-parameters was removed by the port extension after the SOLT calibration. However, the discontinuities due to the SMA transitions still affected measurements. The measured *S*-parameters were converted into the ABCD parameters, and α and β were calculated as real and imaginary parts of the γ (2). The Debye parameters (Table 1) were extracted for both lines using the GA procedures. The real and the imaginary parts of the corresponding relative permittivity, including effective conductivity of the dielectrics, are plotted in Fig. 4.

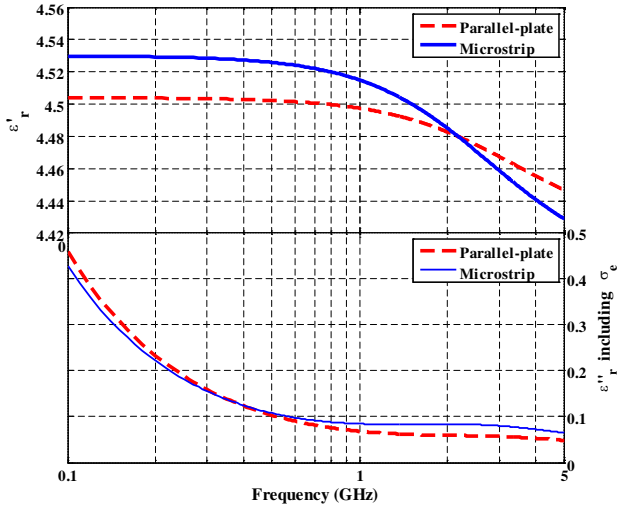

Figure 4. Real and imaginary parts of the extracted permittivity from the parallel-plate and the microstrip structures.

Table 1. Extracted Debye parameters for parallel-plate and microstrip transmission lines.

Structure	ε_s	ε_∞	τ (ps)	σ_e (mS/m)
Parallel-plate	4.504	4.420	46.37	2.531
Microstrip	4.530	4.398	57.22	2.351

The difference between the extracted permittivity (both real and imaginary parts) for two structures is less than 0.025 in the frequency range of 100 MHz–5 GHz. The differences in the extracted parameters can be explained by some tolerances on geometrical parameters, while building test structures. Besides, though FR-4 samples are very close to each other in their dielectric parameters, they might be not identical because of the inhomogeneity of FR-4. Another source of discrepancy for the extracted dielectric parameters may be associated with the fact that in the extraction procedure the conductor surface roughness has been neglected, and the contribution of conductor roughness depends on the geometry of the line.

This comparison verifies the consistency of the proposed method since both the test structures are cut from the same FR-4 sample sheet, and validates the Debye parameter extraction. The extracted Debye parameters (Table 1) are then used in the FDTD (finite-difference time-domain) numerical model for the corresponding parallel-plate and

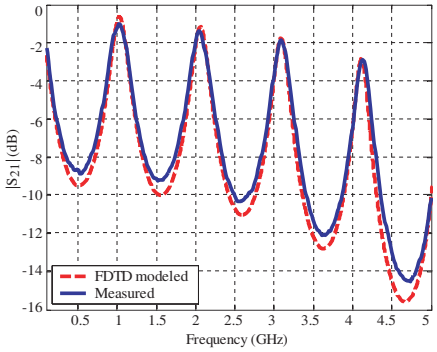

Figure 5. $|S_{21}|$ comparison between the measurement and the full-wave modeling for the parallel-plate transmission line.

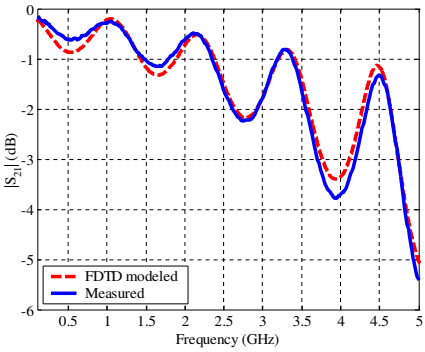

Figure 6. $|S_{21}|$ comparison between the measurement and the full-wave modeling for the microstrip transmission line.

microstrip lines. The SMAs are modeled as thin-wires [44], and the surface impedance boundary condition algorithm is used to model the conductor loss [45]. Figs. 5 and 6 show that the maximum difference between the FDTD simulated and measured $|S_{21}|$ for both the parallel-plate structure and the microstrip structure in the frequency range from 100 MHz to 5 GHz is less than 1 dB. The SMA port effects are partially included in the extracted Debye parameters, and this may lead to discrepancy between the full-wave modeling and the measurements.

4.2. Stripline

A TRL calibration pattern and a test line for the study of stripline structure are designed in an 8-layer PCB on layer 5 with solid reference plane on layers 4 and 6. Three line standards are built to support three different frequency bands of 200 MHz–930 MHz, 930 MHz–4.3 GHz, and 4.3 GHz–20 GHz. The PCB board dimensions are 264 mm (length) $\times$ 248 mm (width) $\times$ 2.69 mm (thickness). The total length of the stripline after moving the TRL calibration reference plane back into the test line is 202.6 mm. The cross-sectional dimensions of the test line, referring to Fig. 3, are $t = 0.03$ mm, $b = 0.75$ mm, $w = 0.32$ mm, $d = 7.3$ mm and $s = 0.007$ mm. The frequency range of interest is from 200 MHz to 20 GHz. According to [46, 47], the calculated cut-off frequency of the first higher-order mode of the stripline is 82 GHz, and the stripline supports TEM wave propagation over the entire frequency range of interest.

Table 2. Extracted two-term Debye parameters for the stripline.

ε_{s1}	ε_{s2}	τ_1 (ps)	τ_2 (ps)	ε_∞	σ_e (mS/m)
4.081	4.068	82.12	5.712	3.95	1.136

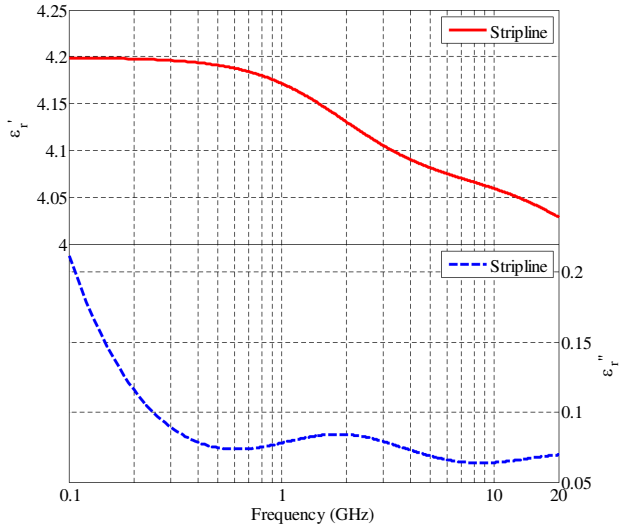

Figure 7. Real and imaginary parts of the extracted permittivity from the stripline structure.

The measurement was performed on an *HP 8720ES* VNA with *ATN-4112 S*-parameter test set. The TRL calibration was implemented before the measurement. The number of sampling points was 201, 801, and 1601, for the frequency spans of 200 MHz–930 MHz, 930 MHz–4.3 GHz, and 4.3 GHz–20 GHz, respectively. The total number of sampling points was 2601 over the entire frequency range of interest, which was sufficient for GA extraction. Since a TRL calibration is based on the standards of "Through", "Reflect", and "Line" to characterize the error model including both VNA and the test structure, errors due to the imperfections of "Short", "Open", and "Load" used in the SOLT calibration are excluded from measurements. Moreover, the TRL calibration moves the measurement reference plane inside the structure under test. The higher-order modes and port parasitics are eliminated from the measurements. For the stripline case, the measurement reference plane is moved 0.5 inch inside of the test line at each end from the SMA centre conductor. The extracted two-term Debye parameters and the effective conducting σ_e for the

substrate material are given in Table 2, and the real and the imaginary parts of the extracted permittivity are plotted in Fig. 7.

These Debye parameters are used in a full-wave simulation tool, which is the CST Microwave Studio realized on the finite integration technique (FIT) [48]. The magnitude and phase of S_{21} obtained by the numerical simulation and measurements are shown in Figs. 8 and 9, respectively. The maximum difference of the $|S_{21}|$ is less than 0.7 dB over the frequency range up to 20 GHz, and the phases almost coincide. This comparison validates the correctness of the extracted Debye parameters and confirms that the proposed method works well. In this extraction, the port effects are removed.

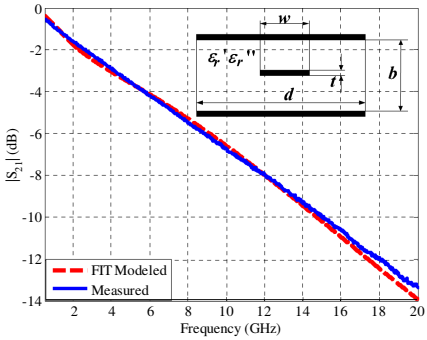

Figure 8. $|S_{21}|$ comparison between the measurement and the full-wave modeling for the stripline structure.

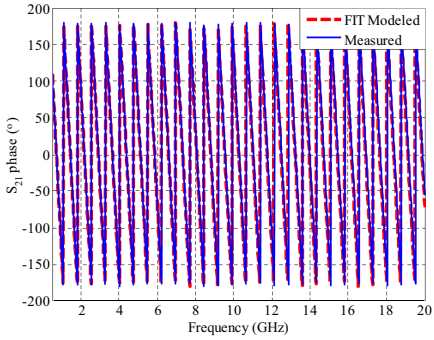

Figure 9. S_{21} phase comparison between the measurement and the full-wave modeling for the stripline structure.

5. CONCLUSIONS

The presented approach to extract Debye parameters for dispersive dielectric substrates in planar transmission line structures is based on approximating complex propagation constant by tuning the Debye parameters in the analytical/empirical models for a dielectric. Dielectric and conductor loss, obtained from measured S-parameters, serve as target data to be approximated in a genetic algorithm. Parameter extraction for both one- and two-term Debye dependencies has been tested in the study. Full-wave FDTD/FIT modeling that used the extracted Debye terms and the measurements were compared, and good agreement was achieved. The proposed approach is straightforward and convenient to use. However, the accuracy of the extracted Debye parameters is directly related to the accuracy of the

S-parameters measurement, which can be seen from the 5-GHz and the 20-GHz test cases. In the 5-GHz case (parallel-plate and microstrip), port effects are partially embedded in the extracted Debye parameters, and the maximum difference between the measured and the full-wave modeled $|S_{21}|$ is of 1 dB. For the 20-GHz case (stripline), port effects are de-embedded from the Debye parameters, and the maximum difference seen is 0.7 dB up to 20 GHz for $|S_{21}|$.

REFERENCES

1. Nikellis, K., N. K. Uzunoglu, Y. Koutsoyannopoulos, and S. Bantas, "Full-wave modeling of stripline structures in multilayer dielectrics," *Progress In Electromagnetics Research*, PIER 57, 253–264, 2006.
2. Wu, B. and L. Tsang, "Full-wave modeling of multiple vias using differential signaling and shared antipad in multilayered high speed vertical interconnects," *Progress In Electromagnetics Research*, PIER 97, 129–139, 2009.
3. Bernardi, P., R. Cicchetti, G. Pelosi, A. Reatti, S. Selleri, and M. Tatini, "An equivalent circuit for EMI prediction in printed circuit boards featuring a straight-to-bent microstrip line coupling," *Progress In Electromagnetics Research B*, Vol. 5, 107–118, 2008.
4. Saito, S. and K. Kurokawa, "A precision resonance method for measuring dielectric properties of low-loss solid materials in the microwave region," *Proceedings of the IRE*, Vol. 44, No. 1, 35–42, 1956.
5. Du, S., "A new method for measuring dielectric constant using the resonant frequency of a patch antenna," *IEEE Trans. Microw. Theory Tech.*, Vol. 34, No. 9, 923–931, Sep. 1986.
6. Abdulnour, J., C. Akyel, and K. Wu, "A generic approach for permittivity measurement of dielectric materials using a discontinuity in a rectangular waveguide or a microstrip line," *IEEE Trans. Microw. Theory Tech.*, Vol. 43, No. 5, 1060–1066, 1995.
7. Holzman, E. L., "Wideband measurement of the dielectric constant of an FR4 substrate using a parallel-coupled microstrip resonator," *IEEE Trans. Microw. Theory Tech.*, Vol. 54, No. 7, 3127–3130, 2006.
8. Huang, J., K. Wu, and C. Akyel, "Characterization of highly dispersive materials using composite coaxial cells, electromagnetic

analysis and wideband measurement," *IEEE Trans. Microw. Theory Tech.*, Vol. 44, No. 5, 770–777, 1996.

9. Baker-Jarvis, J., M. D. Janezic, B. F. Riddle, R. T. Johnk, P. Kabos, C. L. Holloway, R. G. Geyer, and C. A. Grosvenor, "Measuring the permittivity and permeability of lossy materials: Solid, metals, building materials, and negative-index materials," NIST Technical Note 1536, Boulder, CO, USA, Dec. 2004.
10. Afsar, M. N., J. B. Birch, and R. N. Clarke, "The measurement of the properties of materials," *Proc. IEEE*, Vol. 74, No. 1, 183–199, 1986.
11. Klein, K. and J. C. Santamarina, "Methods for broad-band dielectric permittivity measurements (Soil-Water Mixtures, 5 Hz to 1.3 GHz)," *Geotechnical Testing Journal*, Vol. 20, No. 2, Jun. 1997.
12. Deutsch, A., T. Winkel, G. V. Kopcsay, C. W. Surovic, B. J. Rubin, G. A. Katopis, B. J. Chamberlin, and R. S. Krabbenhoft, "Extraction of $\varepsilon_r(f)$ and $\tan\delta(f)$ for printed circuit board insulatiors up to 30 GHz using the short-pulse propagation technique," *IEEE Trans. Adv. Packag.*, Vol. 28, No. 1, 4–12, Feb. 2005.
13. Zhang, J., M. Y. Koledintseva, J. L. Drewniak, D. J. Pommerenke, R. E. DuBroff, Z. Yang, W. Chen, K. N. Rozanov, G. Antonini, and A. Orlandi, "Reconstruction of dispersive dielectric properties for PCB substrates using a genetic algorithm," *IEEE Trans. Electromagn. Compat.*, Vol. 50, No. 3, 704–714, Aug. 2008.
14. Zhang, J., M. Y. Koledintseva, D. P. Pommerenke, J. L. Drewniak, K. N. Rozanov, G. Antonini, and A. Orlandi, "Extraction of dispersive material parameters using vector network analysers and genetic algorithms," *Proc. IEEE Instrumentation and Measurement Technology Conference*, 462–467, Sorrento, Italy, Apr. 2006.
15. Hilfer, R., "H-function representation for stretched exponential relaxation and non-Debye susceptibilities in glassy systems," *Phys. Rev. E*, Vol. 65, 061510, 2002.
16. Jonscher, A. K., *Dielectric Relaxation in Solids*, Chelsea Dielectric Press, 1983.
17. Djordjevic, A. R., R. M. Biljic, V. D. Likar-Smiljanic, and T. K. Sarkar, "Wideband frequency-domain characterization of FR-4 and time-domain causality," *IEEE Trans. on Electromag. Compat.*, Vol. 43, No. 4, 662–667, Nov. 2001,
18. Koledintseva, M. Y., J. Wu, J. Zhang, J. L. Drewniak, and K. N. Rozanov, "Representation of permittivity for multi-phase dielectric mixtures in FDTD modeling," *Proc. IEEE Symp.*

Electromag. Compat., Vol. 1, 309–314, Santa Clara, CA, USA, Aug. 2004.

19. Koledintseva, M. Y., K. N. Rozanov, A. Orlandi, and J. L. Drewniak, "Extraction of the Lorentzian and Debye parameters of dielectric and magnetic dispersive materials for FDTD modeling," *J. Electr. Eng., IEE Slovak*, Vol. 53, No. 9, 97–100, 2002.
20. Landau, L. D. and E. M. Lifshitz, *Electrodynamics of Continuous Media*, 256–265, Pergamon Press, 1960.
21. Rahmat-Samii, Y. and E. Michielssen, *Electromagnetic Optimization by Genetic Algorithms*, 1–93, Wiley, 1999.
22. Haupt, R. L. and D. H. Werner, *Genetic Algorithms in Electromagnetics*, IEEE Press, Wiley, 2007.
23. Mittal, G. and D. Singh, "Critical analysis of microwave specular scattering response on roughness parameter and moisture content for bare periodic rough surfaces and its retrieval," *Progress In Electromagnetics Research*, PIER 100, 129–152, 2010.
24. Liu, B., L. Beghou, L. Pichon, and F. Costa, "Adaptive genetic algorithm based source identification with near-field scanning method," *Progress In Electromagnetics Research B*, Vol. 9, 215–230, 2008.
25. Chen, H. T., G.-Q. Zhu, and S.-Y. He, "Using genetic algorithm to reduce the radar cross section of three-dimensional anisotropic impedance object," *Progress In Electromagnetics Research B*, Vol. 9, 231–248, 2008.
26. Agastra, E., G. Bellaveglia, L. Lucci, R. Nesti, G. Pelosi, G. Ruggerini, and S. Selleri, "Genetic algorithm optimization of high-efficiency wide-band multimodal square horns for discrete lenses," *Progress In Electromagnetics Research*, PIER 83, 335–352, 2008.
27. Xu, Z., H. Li, Q.-Z. Liu, and J.-Y. Li, "Pattern synthesis of conformal antenna array by the hybrid genetic algorithm," *Progress In Electromagnetics Research*, PIER 79, 75–90, 2008.
28. Meng, Z., "Autonomous genetic algorithm for functional optimization," *Progress In Electromagnetics Research*, PIER 72, 253–268, 2007.
29. Zhang, Z., T. Hagfors, E. Nielsen, G. Picardi, A. Mesdea, and J. J. Plaut, "Dielectric properties of the Martian south polar layered deposits: MARSIS data inversion using Bayesian inference and genetic algorithm," *J. Geophys. Res.*, Vol. 113, E05004, May 2008.

30. Diaz-Morcillo, A., J. Monzo-Cabrera, M. E. Requena-Perez, and A. Lozano-Guerrero, "Application of genetic algorithms in the determination of dielectric properties of materials at microwave frequencies," *Lecture Notes in Computer Science (LNCS)*, Vol. 4528, 608–617, Nature Inspired Problem-Solving Methods in Knowledge Engineering, Springer, Berlin, 2007.
31. Oswald, B., D. Erni, H. R. Benedickter, W. Bachtold, and H. Fluhler, "Dielectric properties of natural materials," *IEEE Int. Symp. Antennas and Propagation Society (APS)*, Vol. 4, 2002–2005, Jun. 21–26, 1998.
32. Koledintseva, M. Y., J. L. Drewniak, D. J. Pommerenke, K. N. Rozanov, G. Antonini, and A. Orlandi, "Wide-band Lorentzian media in the FDTD algorithm," *IEEE Trans. on Electromag. Compat.*, Vol. 47, No. 2, 392–398, May 2005.
33. Koul, A., P. K. R. Anmula, M. Y. Koledintseva, J. L. Drewniak, and S. Hinaga, "Improved technique for extracting parameters of low-loss dielectrics on printed circuit boards," *Proc. IEEE Symp. Electromag. Compat.*, 191–196, Austin, TX, Aug. 17–21, 2009.
34. Braunisch, H., X. Gu, A. Camacho-Bragado, and L. Tsang, "Off-chip rough-metal-surface propagation loss modeling and correlation with measurements," *IEEE Electronic Components and Technology Conference*, 785–791, 2007.
35. Koledintseva, M. Y., A. Koul, P. K. R. Anmula, J. L. Drewniak, S. Hinaga, E. Montgomery, and K. N. Rozanov, "Separating dielectric and conductor loss for rough striplines in printed circuit boards," *Progress In Electromagnetics Research Symposium Abstracts*, 213, Moscow, Russia, Aug. 18–21, 2009.
36. Janezic, M. D. and J. A. Jargon, "Complex permittivity determination from propagation constant measurements," *IEEE Microwave and Guided Wave Letters*, Vol. 9, No. 2, 76–78, Feb. 1999.
37. Baker-Jarvis, J., E. Vanzura, and W. Kissick, "Improved technique for determining complex permittivity with the transmission/reflection method," *IEEE Trans. Microw. Theory Techn.*, Vol. 38, 1096–1103, Aug. 1990.
38. Hoffman, R. K., *Handbook of Microwave Integrated Circuits*, Artech House, 1987.
39. Pozar, M., *Microwave Engineering*, 2nd edition, Wiley, 1998.
40. Schneider, M. V., "Microstrip lines for microwave integrated circuits," *The Bell System Technical Journal*, Vol. 48, No. 5–6, 1421–1444, 1969.

41. Gardiol, F. and K. Chang, *Microstrip Circuits*, 33–58, Wiley, 1994.
42. Wheeler, H. A., "Transmission line properties of a strip on a dielectric sheet on a plane," *IEEE Trans. Microw. Theory Tech.*, Vol. 25, No. 8, 631–647, 1977.
43. Wadell, B. C., *Transmission Line Design Handbook*, 129–131, Artech House, 1991.
44. Hockanson, D. M., J. L. Drewniak, T. H. Hubing, and T. P. van Doren, "FDTD modeling of thin wires simulating common-mode radiation from structures with attached cables," *Proc. IEEE Symp. Electromag. Compat.*, 168–173, Atlanta, GA, USA, Aug. 1995.
45. Wang, C., J. L. Drewniak, and M. Li, "FDTD modeling of skin effect," *Proc. IEEE Symp. Electromag. Compat.*, 246–249, Beijing, China, May 2002.
46. Mongia, R., I. Bahl, and P. Bhartia, *RF and Microwave Coupled-Line Circuits*, 83–90, Artech House, 1999.
47. Zhang, J., J. L. Drewniak, D. P. Pommerenke, R. E. DuBroff, Z. Yang, W. Cheng, J. Fisher, and S. Camerlo, "Signal link-path characterization up to 20 GHz based on a stripline structure," *Proc. of the 2006 IEEE International Symposium on Electromagnetic Compatibility*, Vol. 2, 356–361, Portland, OR, Aug. 2006.
48. Clemens, M., S. Drobny, and T. Weiland, "Time integration of slowly-varying electromagnetic field problems using the finite integration technique," *Scientific Computing in Electrical Engineering*, U. van Reinen, M. Guenther, and Hecht (eds.), 63–70, Springer Verlag, 2001.